Effects of spatial and temporal noise on a cubic-autocatalytic reaction-diffusion model

Jean-Sébastien Gagnon,[1,*] David Hochberg,[2,†] and Juan Pérez-Mercader[1,3,‡]
[1]*Department of Earth and Planetary Sciences, Harvard University, Cambridge, Massachusetts, USA*
[2]*Centro de Astrobiología (CSIC-INTA), Madrid, Spain*
[3]*Santa Fe Institute, Santa Fe, New Mexico, USA*
(Received 8 December 2016; published 3 March 2017)

We characterize the influence that external noise, with both spatial and temporal correlations, has on the scale dependence of the reaction parameters of a cubic autocatalytic reaction diffusion (CARD) system. Interpreting the CARD model as a primitive reaction scheme for a living system, the results indicate that power-law correlations in environmental fluctuations can either decrease or increase the rates of nutrient decay and the rate of autocatalysis (replication) on small spatial and temporal scales.

DOI: 10.1103/PhysRevE.95.032106

I. INTRODUCTION

Any realistic chemical or biological system is in contact and interacts with an environment that can affect its evolution in important ways. The environment can be either deterministic (e.g., periodic forcing) or stochastic (e.g., fluctuations in temperature or concentration). In this general context, two types of questions are worth contemplating. First, is it possible to compute or measure the effect of the environment on the behavior and evolution of a chemical or biological system? Studying that question might have applications in various domains, such as noisy gene expression in cells (see, for example, Ref. [1]) and origins of life research [2,3]. Second, is it possible to probe or control a chemical or biological system by manipulating its environment? Possible applications of research along those lines include probing underlying mechanisms in chemical reactions using various perturbations (deterministic environment) [4], noise-controlled transitions in chemical systems [5–8], and control of artificial self-organized systems in bioengineering [9].

Reaction-diffusion equations can be used to model various phenomena ranging from (biological) pattern formation [10–13], ecological invasions [14], tumor growth [15], and oscillating chemical reactions [12,16]. Of particular interest is the cubic autocatalytic reaction-diffusion (CARD) model [7,17], based on a two-species autocatalytic chemical reaction [18–23]. Numerical simulations of the deterministic [17] and stochastic [7] CARD model show the appearance of self-replicating domains that are analogous to simple cells. This makes the CARD model a very interesting nontrivial simplified model for carrying out both analytic and numerical studies of primitive analogs of living organisms. In the following, we focus on studying the effects of a stochastic environment on the behavior of the CARD model. This type of environment can be modeled by adding a noise term to the CARD evolution equations.

In order to get a quantitative handle on these phenomena, application of the renormalization group is ideally suited. One then obtains flow equations which indicate how certain model parameters can change with the scale of the observation (or the scale of the probe employed to such end) due to fluctuations. Our aim is to get a better understanding of how correlations in external noise modify the parameters appearing in simple chemical reaction models. This way it is possible to either study the effect of the environment on analog living systems or get clues about underlying chemical mechanisms using external noise.

In previous works [24,25], we investigated the small-scale properties of the stochastic CARD model due to the presence of environmental fluctuations using field-theoretical and renormalization techniques. Some technical aspects, having to do with regularization procedures, made this analysis more intricate than would have been naively expected, so we focused our investigation on noise with only power-law correlations in space. In this paper, we extend our analysis to noise with both spatial and temporal power-law correlations.

The remainder of this paper is organized as follows. In Sec. II we briefly present the CARD model and some of its properties. We then discuss one-loop corrections to the parameters of the model and the corresponding β function in Sec. III. We consider the effect of fluctuations on the parameters in Sec. IV. We finally conclude in Sec. V. Feynman rules and technical details related to the computation of one-loop corrections are relegated to the Appendices.

II. THE STOCHASTIC CARD MODEL

The CARD model [7,17] is based on the following chemical reactions [18–23]:

$$\begin{aligned} \mathrm{U} + 2\mathrm{V} &\xrightarrow{\lambda} 3\mathrm{V}, \\ \mathrm{V} &\xrightarrow{r_v} \mathrm{P}, \\ \mathrm{U} &\xrightarrow{r_u} \mathrm{Q}, \\ &\xrightarrow{f} \mathrm{U}. \end{aligned} \tag{1}$$

A substrate U (viewed as the "food" in the living system interpretation of the CARD model) is fed into the system at a constant rate f. The species V (viewed as the "organism") consumes the substrate U and turns it into V via an autocatalytic reaction with rate constant λ. This autocatalytic reaction embodies a crude form of metabolism. In numerical simulations, the species V forms cell-like domains over the

*gagnon01@fas.harvard.edu
†hochbergd@cab.inta-csic.es
‡jperezmercader@fas.harvard.edu

substrate U in a certain parameter range. Both species V and U decay into inert products P and Q with decay rates r_v and r_u.

The space-time evolution of the chemical concentrations $U(\mathbf{x},t)$ and $V(\mathbf{x},t)$ in the general case where diffusion and noise are present is governed by the following equations:

$$\frac{\partial V}{\partial t} = D_v\nabla^2 V - r_v V + \lambda U V^2 + \eta_v(x), \tag{2}$$

$$\frac{\partial U}{\partial t} = D_u\nabla^2 U - r_u U - \lambda U V^2 + \eta_u(x) + f, \tag{3}$$

where we use the shortcut notation $x = (\mathbf{x},t)$, $U = U(\mathbf{x},t)$, $V = V(\mathbf{x},t)$, and D_u and D_v are the diffusion constants of the chemical species U and V, respectively. The terms $\eta_u(x)$ and $\eta_v(x)$ are additive space-time-dependent noises discussed in more detail below. Note that the use of concentrations is a reasonable approach when the number of molecules per unit volume varies smoothly (differentiably) from one spatial point to another and from one time to another. Concentrations result from averaging the number of molecules over spatial and temporal domains. We implicitly assume we are in chemical or physical situations where this averaging procedure can be applied meaningfully (i.e., we do not consider either extremely dilute systems nor systems having very small numbers of molecules). We come back to this point in Sec. IV.

For simplicity, we work in an approximation where $U \gg 2f/r_u$. In such a case, the feeding term f in Eq. (3) can be neglected [24]. This approximation is generally valid when the initial amount of food in the system U_0 is large compared to the equilibrium value $U_{\rm eq} = f/r_u$, in which case the effects of feeding are negligible. This can be seen as follows. The amount of substrate U present in the system decreases via decay into inert products or via conversion into V. When $U_0 \gg U_{\rm eq}$, there is a sufficient quantity of substrate U in the reaction domain that the system evolves without need for external feeding (f). Since interactions are generally small, the main source of loss of U is via exponential decay. When the initial amount of U at time t is comparable to the equilibrium value, $U_0 e^{-r_u t} \approx U_{\rm eq}$, then this approximation breaks down. This happens on a time scale $t > r_u^{-1}\ln(U_0/U_{\rm eq})$. Up to this time scale, the system can be regarded as being out of equilibrium, and so the living system interpretation of the CARD model should still be valid. In practice, neglecting f amounts to neglecting one tadpole diagram at one-loop.

The effect of the environment on the CARD dynamics is modeled by adding space-time-dependent noise terms as indicated in Eqs. (2) and (3). In general, noise terms can be either additive or multiplicative, depending on which external parameter is fluctuating. For example, if the autocatalytic reaction in the CARD model is light sensitive and the system driven by a fluctuating light source, then $\lambda U V^2 \to \lambda[\eta]UV^2$ and the noise is multiplicative. On the other hand, if the amount of food present in the environment fluctuates, then $f \to f + \eta$ and the noise enters additively into the U equation. We are aware that if the CARD model is viewed as a very primitive analog of a living system, then from a "biological" point of view it is harder to justify additive noise for the V equation. But although we use the CARD model because of its rich phenomenology and its potential use as a living system analog, this is only one class of applications of the methods presented in this paper. As explained in the Introduction, in applications where the environment is used to probe or control a chemical system, the choice of noise to be included depends on experimental constraints and on how the experiment is designed. In such applications, it is easier to justify additive noise.

Noise correlations in the environment may have various effects on chemical and biological systems. It thus makes sense to pick a form for the noise that is chemically or biologically relevant (although experiments designed to probe or control a specific chemical or biological system are free to choose any type of noise). Completely uncorrelated (i.e., Gaussian white) noise is often used in applications for its mathematical simplicity, although there exist examples of correlated noise in chemistry and biology. For instance, anomalous diffusion of macroscopic molecules in some living systems [26,27] may imply that the "chemical food" available to a cell fluctuates in a power-law fashion. Similarly, the authors of Ref. [28] review the evidence that active transport through cell membranes is noisy with power-law correlations in space and time, which again may imply that the inflow of chemicals inside the cell fluctuates. Power-law noise (which includes white noise as a special case) thus seems a biologically relevant stochastic environment. From a practical point of view, power laws can also be used as a basis for Taylor expanding more complex noise functions.

In the following, we use a three-parameter (an amplitude plus two power-law exponents) Gaussian noise with both spatial and temporal power-law correlations [29] to describe the stochastic component in Eqs. (2) and (3). Its statistical properties are given by:

$$\langle\eta_v(k)\rangle = \langle\eta_u(k)\rangle = 0, \tag{4}$$

$$\langle\eta_v(k)\eta_v(p)\rangle = 2A_v|\mathbf{k}|^{-y_v}\omega^{-2\theta_v}(2\pi)^{d_s+1}\delta^{(d_s+1)}(k+p), \tag{5}$$

$$\langle\eta_u(k)\eta_u(p)\rangle = 2A_u|\mathbf{k}|^{-y_u}\omega^{-2\theta_u}(2\pi)^{d_s+1}\delta^{(d_s+1)}(k+p), \tag{6}$$

$$\langle\eta_v(k)\eta_u(p)\rangle = \langle\eta_u(k)\eta_v(p)\rangle = 0, \tag{7}$$

where we use the shortcut notation $k = (\mathbf{k},\omega)$ and we have expressed the correlations in Fourier space for later convenience. All higher-order moments are zero (Gaussian noise) and d_s is the dimension of space. The noise amplitudes $A_u, A_v > 0$ are free parameters of the model and give the overall strength of the fluctuations. The spatial noise exponents y_u, y_v and temporal noise exponents θ_u, θ_v are also free parameters of the model that give the strength of correlations as a function of wave number and frequency. The case of pure spatial correlations ($\theta_u = 0$, $\theta_v = 0$) is treated in Ref. [24]. In this paper, we study the more general case where both spatial and temporal correlations can be present and acting together.

Note that the additive noise terms in Eqs. (2) and (3) are examples of extrinsic noise, i.e., noise caused by the application of a random force external to the system [30]. Intrinsic noise is another generic type of noise that is present even for systems in complete isolation. It is generally attributed to the fact that chemical systems are made of discrete particles and

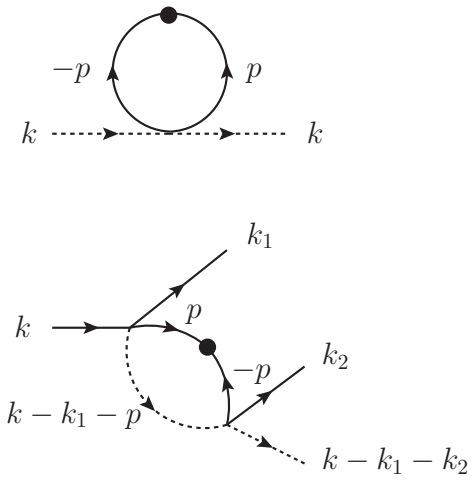

FIG. 1. One-loop diagrams contributing to r_u (top) and λ (bottom), in the approximation $U \gg 2f/r_u$.

quantum mechanical randomness [30]. On physical grounds, we expect intrinsic noise to be negligible in macroscopic systems at relevant experimental temperatures, in the same way that quantum fluctuations are negligible compared to thermal fluctuations in high-temperature condensed matter systems. In situations where discretization effects are not negligible, both types of noise must be taken into account. This can be done using a master equation approach (e.g., Refs. [30–32]), which lies beyond the scope of this paper.

III. UV RENORMALIZATION OF THE STOCHASTIC CARD MODEL

We are interested in the effects of spatially and temporally correlated noise on the small-scale properties of the CARD model's dynamics. To do that, we use the renormalization group and run it from large to small scales, or from the infrared (IR) to the ultraviolet (UV). The change in model parameters induced by fluctuations is encoded in β functions, thus our goal is to compute those β functions at one-loop in perturbation theory. Since this type of computation has been carried out in detail for spatially correlated noise in Ref. [24], we focus here on the modifications and differences when including explicit temporal correlations.

A. One-loop corrections to the parameters

β Functions are computed from the UV divergence structure of Feynman diagrams. The Feynman rules corresponding to the CARD equations (2) and (3) are discussed in Refs. [24,29] and summarized in Appendix A. At one-loop order, the only nontrivial corrections to the model parameters are shown in Fig. 1 [24].

To illustrate the differences between the cases with and without temporally correlated noise, consider the one-loop correction to the decay rate r_u. In d_s spatial dimensions, the correction is given by:

$$\begin{aligned}\Gamma_{r_u}(0) &= -2\lambda A_v \int \frac{d^{d_s}p}{(2\pi)^{d_s}} \int \frac{d\omega}{(2\pi)}\, \omega^{-2\theta_v} |\mathbf{p}|^{-y_v} \\ &\quad \times \left(\frac{1}{D_v|\mathbf{p}|^2 - i\omega + r_v}\right)\left(\frac{1}{D_v|\mathbf{p}|^2 + i\omega + r_v}\right), \\ &= -2\lambda A_v \int \frac{d^{d_s}p}{(2\pi)^{d_s}} \int \frac{d\omega}{(2\pi)}\, \omega^{-2\theta_v} |\mathbf{p}|^{-y_v} \\ &\quad \times \left[\frac{1}{\omega^2 + (D_v|\mathbf{p}|^2 + r_v)^2}\right], \end{aligned} \tag{8}$$

where we have taken all external momenta and frequencies to be zero (this is sufficient for β-function computations). Contrary to quantum field theory, there is no Lorentz invariance in the CARD model, and thus the integrals over the frequency and wave number in Eq. (8) must be carried out separately. Depending on the dimension of space d_s and on the parameters of the model y_v and θ_v, the momentum, the frequency, or even both integrals may diverge. We use dimensional continuation as our regulator (see Ref. [24] for a discussion on the use of dimensional regularization in the presence of power-law noise). Analytically continuing the space dimension to d and the time dimension to z, we obtain:

$$\begin{aligned}\Gamma_{r_u}(0) &= -2\lambda^{(d)} A_v^{(d,z)} \int \frac{d^d p}{(2\pi)^d} \int \frac{d^z\omega}{(2\pi)^z}\, |\omega|^{-2\theta_v} |\mathbf{p}|^{-y_v} \\ &\quad \times \left[\frac{1}{|\omega|^2 + (D_v|\mathbf{p}|^2 + r_v)^2}\right], \end{aligned} \tag{9}$$

where $\lambda^{(d)}$ and $A_v^{(d,z)}$ are the rate constant and noise amplitude in d spatial and z time dimensions, respectively. Simple power counting shows that the one-loop correction behaves as:

$$\Gamma_{r_u} \sim \Lambda^{d-y_v+2z-4\theta_v-4}, \tag{10}$$

where Λ is a large momentum scale cutoff. For convenience, we define the following parametrization:

$$\frac{d}{2} - \frac{y_v}{2} = m - \frac{\epsilon}{2} \quad m = 1,2,3,\ldots \tag{11}$$

$$\frac{z}{2} - \theta_v = \frac{(n+1)}{2} - \frac{\delta}{2} \quad n = 0,1,2,3,\ldots \tag{12}$$

with $0 < \epsilon < 2$ and $0 < \delta < 1$, giving:

$$\Gamma_{r_u} \sim \Lambda^{2m+2n-2-(\epsilon+2\delta)}. \tag{13}$$

The integers m and n define the order of the divergence (logarithmic, quadratic) and ϵ and δ the (fractional) distance from some critical dimension [33]. Note that we are interested in the small-scale properties of the CARD model and thus in UV divergences, hence the restrictions on m and n (non-negative values) in Eqs. (11) and (12). Note also that the divergence structure of Γ_{r_u} depends on m and n, implying that it can be controlled externally via the noise exponents y_v and θ_v.

The correction Γ_{r_u} is logarithmically divergent for ($m = 1, n = 0$). This case corresponds to purely spatial power-law noise and is treated in Ref. [24]. Note that it is not possible to get a logarithmically divergent correction to r_u from purely temporal power-law noise (i.e., $m = 0$, $n = 1$), since $m = 0$ corresponds to IR divergences [24] that are not the focus of

the present study. There are two ways to obtain a quadratically divergent correction to r_u. The first way is by setting ($m = 2$, $n = 0$), corresponding to purely spatial power-law noise and treated in Ref. [24]. The second way is by setting ($m = 1, n = 1$), and is the first nontrivial case involving a mixture of spatial and temporal power-law noise. Higher-order divergences are obtained when $m + n > 2$; however, their treatment is more subtle and requires the introduction of higher-order terms in Eqs. (2) and (3), as discussed in Refs. [24,25]. In the following, we focus on the ($m = 1, n = 1$) case and leave the consideration of higher-order divergences for a future work.

Integrating Eq. (9) over frequency using the method of dimensional regularization in the presence of noise [24], we obtain:

$$\Gamma_{r_u}(0) = -\lambda^{(d)} A_v^{(d,z)}\, K_z\, \Gamma\left(-\frac{z}{2}+\theta_v+1\right)\Gamma\left(\frac{z}{2}-\theta_v\right) \times \int \frac{d^d p}{(2\pi)^d}\, |\mathbf{p}|^{-y_v} \frac{1}{(D_v|\mathbf{p}|^2 + r_v)^{-z+2\theta_v+2}}, \quad (14)$$

where $K_z \equiv 2/[(4\pi)^{\frac{z}{2}}\Gamma(\frac{z}{2})]$. We see from Eq. (14) that the frequency and momentum integrals mix in a nontrivial way due to the presence of θ_v in the exponent of $(D_v|\mathbf{p}|^2 + r_v)$. The momentum integral is performed in a similar fashion, giving:

$$\Gamma_{r_u}(0) = -\frac{\lambda^{(d)} A_v^{(d,z)}}{2 D_v^{-z+2\theta_v+2}} K_d K_z\, \Gamma\left(-\frac{z}{2}+\theta_v+1\right)\Gamma\left(\frac{z}{2}-\theta_v\right) \times \frac{\Gamma\left(-\frac{d}{2}+\frac{y_v}{2}-z+2\theta_v+2\right)\Gamma\left(\frac{d}{2}-\frac{y_v}{2}\right)}{\Gamma(-z+2\theta_v+2)} \times \left(\frac{r_v}{D_v}\right)^{\frac{d}{2}-\frac{y_v}{2}+z-2\theta_v-2}. \quad (15)$$

We have explicitly checked the commutativity of the two integrals in Eq. (9). Substituting the definitions (11) and (12) (with $m = 1$ and $n = 1$) into Eq. (15) and expanding around the critical dimension $d_c^\lambda = y_v + 2$ we obtain:

$$\Gamma_{r_u}(0) = \frac{2\lambda^{(d_c^\lambda)} A_v^{(d_c^\lambda,1)} r_v}{D_v} K_{d_c^\lambda} K_1\left(\frac{1}{\epsilon + 2\delta}\right). \quad (16)$$

We of course set $z = 1$, corresponding to one temporal dimension. The unusual $1/(\epsilon + 2\delta)$ pole in Eq. (16) is a direct result of the mixing between the frequency and momentum integrals, a feature that does not appear in the purely spatial power-law noise case. It implies that the independent parameters ϵ and δ do not have to be both zero to produce a divergence, only the specific combination $\epsilon + 2\delta$ must vanish. This differs considerably from the purely spatial power-law noise case. A similar one-loop correction can be obtained for the rate constant λ (see the bottom diagram in Fig. 1):

$$\Gamma_\lambda(0) = -8\lambda^2_{(d_c^\lambda)} A_v^{(d_c^\lambda,1)} \frac{D_u}{D_v^2 - D_u^2} \ln\left(\frac{D_v}{D_u}\right) K_{d_c^\lambda} K_1\left(\frac{1}{\epsilon}\right). \quad (17)$$

Details of the computation are presented in Appendix B. Note that the interplay between Γ functions in Eq. (15) may produce unexpected cancellations of poles in the final result. For instance, it is possible to show that $\Gamma_{r_u}(0)$ has no pole and is thus finite for even n and arbitrary m. This unexpected behavior is absent from the purely spatially correlated power-law noise case.

B. β-function computations

In the ($m = 1$, $n = 1$) case, the one-loop correction to the decay rate Γ_{r_u} is divergent when $d_s \geqslant y_v$ and the correction to the rate constant Γ_λ is divergent for $d_s \geqslant y_v + 2$ (when $\epsilon = \delta = 0$). For β-function computation purposes, there are thus three different regimes to distinguish.

1. Regime 1

For $d_s < y_v$, both r_u and λ are finite and do not require renormalization. The β functions are trivial in this regime.

2. Regime 2

For $y_v \leqslant d_s < y_v + 2$, r_u is logarithmically divergent and λ is finite. Thus only r_u requires renormalization and has a nontrivial β function. To study such a regime, we expand around the critical dimension d_c^λ such that $d = d_c^\lambda - (\epsilon + 2\delta)$ (with $\epsilon + 2\delta > 0$). Following standard procedures, we write down the Z factor for r_u:

$$Z_{r_u} = 1 + \frac{\Gamma_{r_u}(0)}{r_u}, \quad (18)$$

$$= 1 + 2g^{(d_c^\lambda,1)} K_d K_1\left(\frac{1}{\epsilon + 2\delta}\right), \quad (19)$$

where the effective coupling $g^{(d,z)}$ is defined as:

$$g^{(d,z)} = \frac{\lambda^{(d)} A_v^{(d,z)} r_v}{D_v r_u}. \quad (20)$$

Note that $g^{(d,z)}$ is dimensionless when $d \to d_c^\lambda$ and $z \to 1$, as it should be. The β function for $g^{(d_c^\lambda,1)}$ can be obtained from Eq. (20):

$$\beta_g \equiv T\frac{dg}{dT} = \frac{1}{2}|\epsilon + 2\delta| g + g^2 K_d K_1, \quad (21)$$

where T is an arbitrary sliding scale and we dropped the $(d_c^\lambda,1)$ superscript to avoid cluttering of indices. To interpret physically, we revert back to the original parameters with a change of variable in Eq. (21), giving:

$$\beta_{r_u} = -\left(\frac{1}{2}|\epsilon + 2\delta| r_u + \frac{\lambda A_v r_v}{D_v} K_d K_1\right). \quad (22)$$

Note that perturbation theory limits the validity of the above result to the region where $g = \lambda A_v r_v / D_v r_u < 1$. Indeed, the β function (22) is obtained by perturbing around the free response functions (A1) and (A2) (corresponding to diffusive solutions). Corrections to the free response functions are due to nonlinearities in the CARD equations and are represented by loop diagrams. For our perturbative solution to be valid, the expansion parameter g must satisfy $g < 1$. In the case where $g > 1$, corrections are larger than the free solutions because nonlinearities are too strong [the same discussion applies to the expansion parameter h, see Eq. (25)]. The CARD model displays a rich phenomenology (stripes, self-replicating domains, etc.), and each type of pattern appears within a certain parameter range. Some types of patterns result from strong nonlinearities, meaning that there is a good chance

that $g > 1$, $h > 1$, and thus perturbation theory is not valid when those patterns are present. The perturbative tools and renormalization techniques used in the present paper are thus limited to a certain parameter range dictated by the criteria $g < 1$ and $h < 1$. Blue regions in Figs. 2–4 are regions in parameter space where perturbation theory is not valid.

3. Regime 3

For $d_s \geqslant y_v + 2$, both r_u and λ and require renormalization. Both have a nontrivial β function. To study this regime we expand around d_c^λ such that $d = d_c^\lambda - (\epsilon + 2\delta)$ (with $\epsilon + 2\delta < 0$). Since both r_u and λ run simultaneously, there is an extra Z factor in addition to Eq. (18):

$$Z_\lambda = 1 + \frac{\Gamma_\lambda(0)}{\lambda}, \tag{23}$$

$$= 1 - 8h^{(d_c^\lambda,1)} \ln\left(\frac{D_v}{D_u}\right) K_{d_c^\lambda} K_1\left(\frac{1}{\epsilon}\right), \tag{24}$$

where the effective coupling $h^{(d,z)}$ is defined as:

$$h^{(d,z)} = \frac{\lambda^{(d)} A_v^{(d,z)} D_u}{\left(D_v^2 - D_u^2\right)}. \tag{25}$$

Using Eqs. (20) and (25), the β functions for the effective couplings $g^{(d_c^\lambda,1)}$ and $h^{(d_c^\lambda,1)}$ can be obtained:

$$\beta_g \equiv T\frac{dg}{dT} = \left(\frac{\epsilon}{2} + \delta\right)g + g^2 K_d K_1 + 8gh \ln\left(\frac{D_v}{D_u}\right) K_d K_1\left(\frac{1}{2} + \frac{\delta}{\epsilon}\right), \tag{26}$$

$$\beta_h \equiv T\frac{dh}{dT} = \left(\frac{\epsilon}{2} + \delta\right)h + 8h^2 \ln\left(\frac{D_v}{D_u}\right) K_d K_1\left(\frac{1}{2} + \frac{\delta}{\epsilon}\right). \tag{27}$$

Changing variables, we finally get the β functions for the decay rate and rate constant in regime 3 in terms of the original parameters:

$$\beta_{r_u} = -\frac{\lambda A_v r_v}{D_v} K_d K_1, \tag{28}$$

$$\beta_\lambda = \left(\frac{\epsilon}{2} + \delta\right)\lambda + 8\lambda^2 \frac{A_v D_u}{\left(D_v^2 - D_u^2\right)} \times \ln\left(\frac{D_v}{D_u}\right) K_d K_1\left(\frac{1}{2} + \frac{\delta}{\epsilon}\right), \tag{29}$$

with $\epsilon + 2\delta < 0$. Perturbation theory limits the validity of the above results to the region where $g = \lambda A_v r_v / D_v r_u < 1$ and $h = \lambda A_v D_u / (D_v^2 - D_u^2) < 1$. Note that there seems to be a potential divergence in β_λ when $\delta \neq 0$ and $\epsilon \to 0$. This is problematic and might signal a missing contribution in the perturbative expansion. Fortunately, this divergence is only apparent and can be understood in the following way. The corrections (16) and (17) diverge when $\epsilon + 2\delta \to 0$ and $\epsilon \to 0$, respectively. Both corrections diverge in regime 3, implying that ϵ and δ must tend to zero simultaneously in this regime. Consequently, the situation $\delta \neq 0$ and $\epsilon \to 0$ does not correspond to regime 3 and thus cannot be included in the analysis of Eq. (29).

IV. RESULTS AND DISCUSSION

In this section we integrate the β functions obtained in Sec. III in order to study the behavior of parameters at smaller scales. We also compare the running solutions to the purely spatial power-law noise case and point out qualitative differences in behavior. The β functions in regime 1 are trivial, and thus we only consider regimes 2 and 3 in the following.

A. Running of parameters in regime 2

The running of the decay rate in regime 2 is obtained by integrating the β function (22). The result is as follows:

$$r_u(T) = \left(r_u(T^*) + \frac{2\lambda A_v r_v}{|\epsilon + 2\delta| D_v} K_d K_1\right)\left(\frac{T}{T^*}\right)^{-\frac{|\epsilon+2\delta|}{2}} - \frac{2\lambda A_v r_v}{|\epsilon + 2\delta| D_v} K_d K_1, \tag{30}$$

where T^* is some time scale at which $r_u(T^*)$ is known and can be measured. The result (30) can be compared to the purely spatial power-law noise case found in Ref. [24] (denoted by a GHP superscript in what follows, which stands for the initials of the authors of Ref. [24]):

$$r_u^{(\mathrm{GHP})}(T) = \left[r_u(T^*) + \frac{\lambda A_v^{(\mathrm{GHP})} r_v K_d}{|\epsilon| D_v^2}\right]\left(\frac{T}{T^*}\right)^{-|\epsilon|/2} - \frac{\lambda A_v^{(\mathrm{GHP})} r_v K_d}{|\epsilon| D_v^2}. \tag{31}$$

We note that Eqs. (30) and (31) are very similar but differ in some aspects. First, there are extra numerical factors appearing in Eq. (30) due to the nontrivial integral over frequency. There is also a factor of D_v absent from Eq. (30) due to the fact that the engineering dimensions of the noise amplitudes A_v and $A_v^{(\mathrm{GHP})}$ differ in both cases. Those changes are quantitative

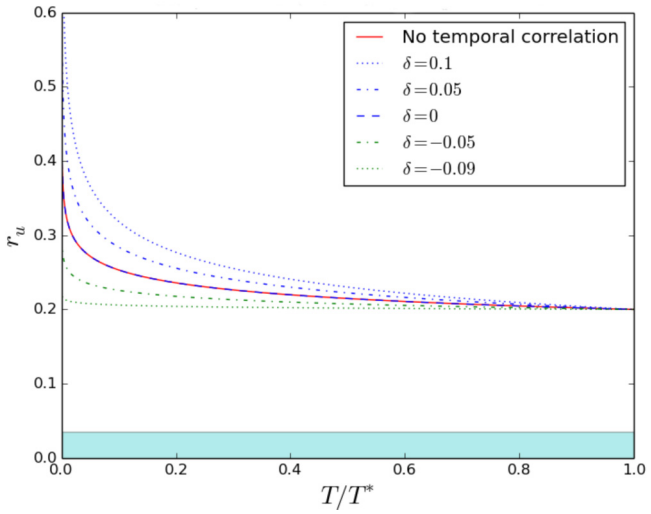

FIG. 2. Running of r_u for regime 2 for different values of δ after effecting the rescaling in Eq. (32). The red line corresponds to the purely spatial correlation case [cf. Eq. (31)]. We used $\epsilon = 0.2$, $D_v = 0.3$, $r_v = 0.4$, $A_v^{(\mathrm{GHP})} = 0.1$, $\lambda = 0.05$, $K_d = 0.05$, $r_u(T^*) = 0.2$ for the plotting. The shaded region indicates the breakdown of perturbation theory.

in nature and do not produce any qualitative changes in the running of the decay rate. They can be eliminated by a simple rescaling of the noise amplitude in the temporally correlated case. Substituting the noise amplitude A_v in Eq. (30) with

$$A_v \to \frac{A_v^{(\mathrm{GHP})}}{2K_1 D_v}, \tag{32}$$

where $A_v^{(\mathrm{GHP})}$ is the noise amplitude in the purely spatial power-law noise case, we obtain:

$$r_u(T) = \left[r_u(T^*) + \frac{\lambda A_v^{(\mathrm{GHP})} r_v}{|\epsilon + 2\delta| D_v^2} K_d\right]\left(\frac{T}{T^*}\right)^{-\frac{|\epsilon+\delta|}{2}} - \frac{\lambda A_v^{(\mathrm{GHP})} r_v}{|\epsilon + 2\delta| D_v^2} K_d. \tag{33}$$

At the pole (i.e., when $\delta = 0$), there is an exact mapping between the purely spatial case (31) and the one with a mixture of spatial and temporal noise correlations (33). Away from the pole (i.e., when $\delta \neq 0$), the behaviors differ, as shown in Fig. 2.

In the living system interpretation of the CARD model, a change in decay rate r_u due to fluctuations implies a change at which nutrient U is removed from the system. Since the growth of an organism (i.e., $\partial V/\partial t$) is proportional to the amount of food present (i.e., $\lambda U V^2$), a larger decay rate implies smaller growth of structures (and vice versa). From Fig. 2, the value of the decay rate is greater or smaller (with respect to the purely spatial case) at shorter scales, depending on the value of δ. This means that temporal correlations can either increase or decrease the running of r_u and thus enhance or suppress the growth of structures at small temporal scales. Note that the running toward small temporal T (or spatial L) scales is in principle limited. At very small scales, the number of U and V molecules in the observed sample is small and does not vary smoothly, implying a breakdown of the description via reaction-diffusion equations. For a mole of molecules, this happens around $T/T^* \sim (L/L^*)^2 \sim 10^{-16}$.

B. Running of parameters in regime 3

The running solutions for the decay rate and rate constant in regime 3 are obtained by integrating the β functions (28) and (29), giving:

$$r_u(T) = r_u(T^*) - \frac{\epsilon}{|\epsilon + 2\delta|}\frac{r_v\left(D_v^2 - D_u^2\right)}{4D_v D_u \ln\left(\frac{D_v}{D_u}\right)} \ln\left\{1 - \frac{8A_v D_u \ln\left(\frac{D_v}{D_u}\right) K_d K_1 \lambda(T^*)}{\epsilon\left(D_v^2 - D_u^2\right)}\left[\left(\frac{T}{T^*}\right)^{-\frac{|\epsilon+2\delta|}{2}} - 1\right]\right\}, \tag{34}$$

$$\lambda(T) = -\frac{\epsilon\left(D_v^2 - D_u^2\right)}{8A_v D_u \ln\left(\frac{D_v}{D_u}\right) K_d K_1}\left[\frac{1}{1 - \left[1 + \frac{\epsilon(D_v^2 - D_u^2)}{8A_v D_u \ln\left(\frac{D_v}{D_u}\right) K_d K_1 \lambda(T^*)}\right]\left(\frac{T}{T^*}\right)^{\frac{|\epsilon+2\delta|}{2}}}\right], \tag{35}$$

with the condition $\epsilon + 2\delta < 0$. Here again T^* is some time scale at which $r_u(T^*)$ and $\lambda(T^*)$ are known. The above running solutions (34) and (35) can be compared to the purely spatial power-law noise results of Ref. [24]:

$$r_u^{(\mathrm{GHP})}(T) = r_u(T^*) + \frac{r_v(D_u + D_v)}{4D_v} \ln\left\{1 + \frac{4A_v^{(\mathrm{GHP})} K_d \lambda(T^*)}{|\epsilon| D_v (D_u + D_v)}\left[\left(\frac{T}{T^*}\right)^{-\frac{|\epsilon|}{2}} - 1\right]\right\}, \tag{36}$$

$$\lambda^{(\mathrm{GHP})}(T) = \frac{|\epsilon| D_v (D_u + D_v)}{4A_v^{(\mathrm{GHP})} K_d}\left\{\frac{1}{1 - \left[1 - \frac{|\epsilon| D_v (D_u + D_v)}{4A_v^{(\mathrm{GHP})} K_d \lambda(T^*)}\right]\left(\frac{T}{T^*}\right)^{\frac{|\epsilon|}{2}}}\right\}. \tag{37}$$

Just as for regime 2, the two sets of running solutions are very similar but differ in some crucial places. Many of those numerical and dimensional factor differences can be eliminated using the following rescaling of the noise amplitude in Eqs. (34) and (35):

$$A_v \to \frac{A_v^{(\mathrm{GHP})}(D_v - D_u)}{2K_1 D_v D_u \ln\left(\frac{D_v}{D_u}\right)}. \tag{38}$$

Doing the above substitution, we get:

$$r_u(T) = r_u(T^*) - \frac{\epsilon}{|\epsilon + 2\delta|}\frac{r_v(D_v + D_u)}{4D_v}\left[\frac{(D_v - D_u)}{D_u \ln\left(\frac{D_v}{D_u}\right)}\right] \ln\left\{1 - \frac{4A_v^{(\mathrm{GHP})} K_d \lambda(T^*)}{\epsilon D_v (D_v + D_u)}\left[\left(\frac{T}{T^*}\right)^{-\frac{|\epsilon+2\delta|}{2}} - 1\right]\right\}, \tag{39}$$

$$\lambda(T) = -\frac{\epsilon D_v (D_v + D_u)}{4A_v^{(\mathrm{GHP})} K_d}\left\{\frac{1}{1 - \left[1 + \frac{\epsilon D_v (D_v + D_u)}{4A_v^{(\mathrm{GHP})} K_d \lambda(T^*)}\right]\left(\frac{T}{T^*}\right)^{\frac{|\epsilon+2\delta|}{2}}}\right\}. \tag{40}$$

When $\delta = 0$ (and taking into account the condition $\epsilon + 2\delta < 0$), we see that Eq. (37) is identical to Eq. (40), showing an exact mapping between the purely spatial and spatial+temporal mixture cases for the rate constant. No such mapping exists

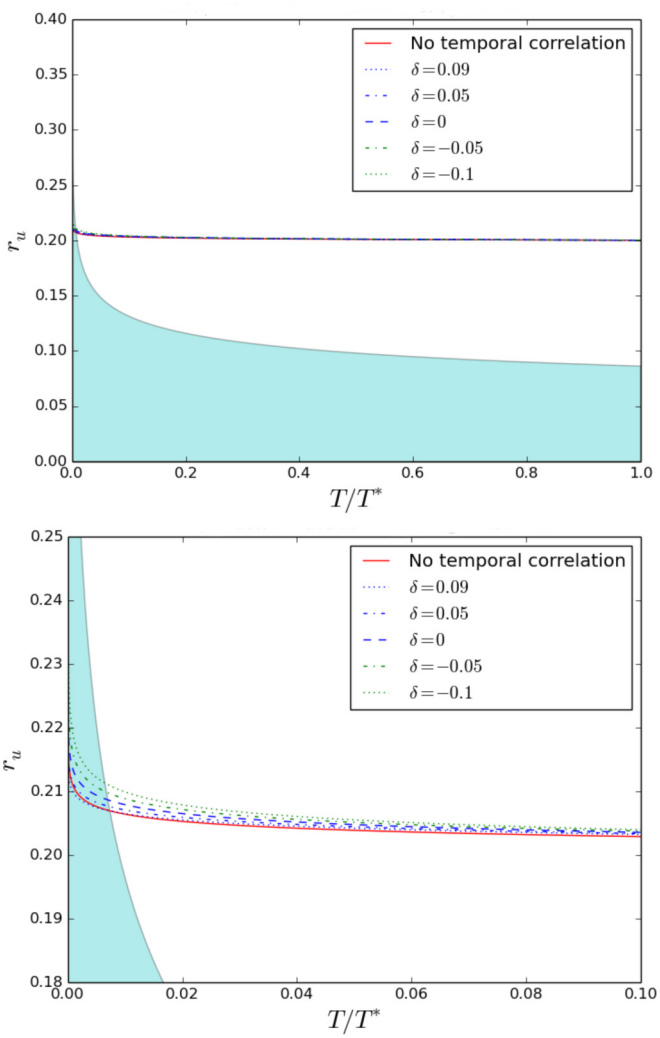

FIG. 3. Top: Running of r_u for regime 3 for different values of δ after doing the rescaling in Eq. (38). The red line corresponds to the purely spatial correlation case [cf. Eq. (36)]. We used $\epsilon = -0.2$, $D_v = 0.3$, $D_u = 0.2$, $r_v = 0.4$, $A_v^{(\mathrm{GHP})} = 0.1$, $K_d = 0.05$, $r_u(T^*) = 0.2$, $\lambda(T^*) = 0.1$ for the plotting. The shaded region indicates the breakdown of perturbation theory. Bottom: Zoom of the top figure.

for the decay rate because of the presence of extra diffusion constant factors that cannot be rescaled away [compare Eqs. (36) and (39)].

Effects of a nonzero δ on the running of the decay rate are small, since the power-law term $(T/T^*)^{-\frac{|\epsilon+2\delta|}{2}}$ is inside a logarithm. This can be seen in Fig. 3. The region where deviations are the largest are in the shaded area where perturbation theory cannot be trusted. Thus we conclude that power-law temporal correlations have a negligible effect on the decay rate in regime 3.

The effect of a nonzero δ on the catalysis rate constant is more pronounced than for the U-decay rate. This can be seen on Fig. 4. In the living system interpretation of the CARD model, a change in constant rate due to fluctuations implies a change in the rate at which new "body parts" are created. Since the growth of an organism (i.e., $\partial V/\partial t$) is proportional

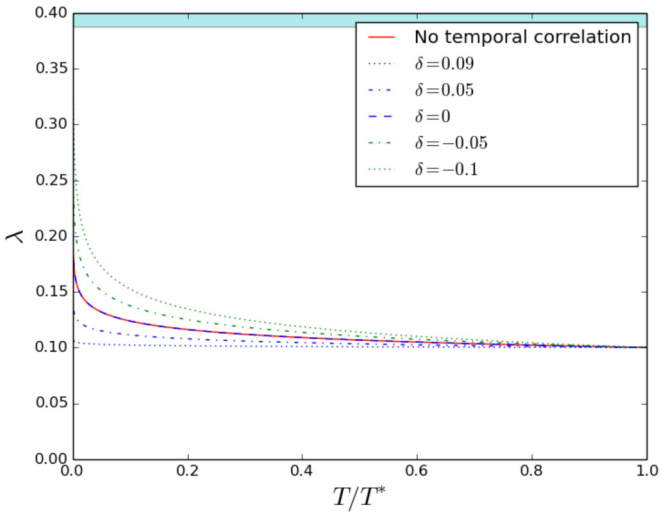

FIG. 4. Running of λ for regime 3 for different values of δ after doing the rescaling in Eq. (38). The red line corresponds to the purely spatial correlation case [cf. Eq. (37)]. We used $\epsilon = -0.2$, $D_v = 0.3$, $D_u = 0.2$, $A_v^{(\mathrm{GHP})} = 0.1$, $K_d = 0.05$, $\lambda(T^*) = 0.1$ for the plotting. The shaded region indicates the breakdown of perturbation theory.

to $\lambda U V^2$, an increase in λ leads to a larger growth of structures (and vice versa). From Fig. 4, we see that the value of the rate constant is larger or smaller at shorter scales with respect to the purely spatial case, depending on the distance from the pole δ. Thus nontrivial temporal correlations can enhance or suppress the growth of structures at small scales.

V. CONCLUSION

In general, large- and small-scale environmental fluctuations can have nontrivial effects on the small-scale, kinetic, and collective properties of chemical systems. In this paper, we have analyzed the effect of noise with both spatial and temporal power-law correlations on the kinetics and phenomenology of a specific cubic autocatalytic reaction-diffusion chemical system. The noise is additive, in that its presence is incorporated as an additive term affecting the individual reaction rates. In particular, using renormalization group techniques, we show analytically how parameters such as chemical decay rates and catalytic rate constants depend on the statistical properties of the noise. The noise causes the model parameters to *renormalize*, that is, to change due to the simultaneous presence of fluctuations and nonlinearities. These noise-induced changes manifest themselves as an inherited and explicit scale dependence of the parameters so affected. Some of these renormalization effects have been studied previously for the case of purely spatial noise in Ref. [24]. Here we found that those effects can be greatly enhanced or suppressed with the presence of temporally correlated noise. We also discuss how, under certain conditions, the effects of spatial and temporal noises can be mapped onto each other.

These results raise important questions regarding the role of external noise in both chemical and biological self-organization and in the environmental selection of reproduc-

tion (catalysis) as well as other dynamical mechanisms. We learn that when describing an open chemical system, not only must we estimate the relevant parameters but also the magnitude of the stochastic influences, the spatial and temporal scales, and the correlations of the latter. The interdependence between an open chemical system and its environment can therefore have important consequences. In the case of nonlinear systems, of which chemical reactions provide immediate examples, the role of noise can be nontrivial by forcing and driving the system to explore new situations which, although not present in the purely deterministic situation, might be favored by external natural selection or enhancement processes and their subsequent pressures. For an adaptive system this can have a direct impact on how the system evolves.

Understanding the effect of external noise on chemical systems can have many applications. One class of applications considers the noise as environmental. Since the reaction-diffusion model studied in this paper can be viewed as a (very simple) generic prototype model for a living system, the techniques developed in the present paper could be used to study its viability [34] under time-dependent environmental pressures. Another class of applications considers the noise as an experimental tool or probe to uncover underlying mechanisms and pathways in chemical systems [25]. The work presented in this paper extends the range of possible noise correlations that can be used to study chemical systems experimentally. The application of the present results to the above problems is a topic of our current research and study.

ACKNOWLEDGMENTS

J.-S.G. and J.P.-M. thank Repsol S.A. for their support. D.H. acknowledges Grant No. CTQ2013-47401-C2-2-P from MINECO (Spain).

APPENDIX A: FEYNMAN RULES

A discussion of Feynman rules for stochastic partial differential equations can be found in Refs. [35,36]. In the present case, they are obtained by iterating the Fourier-transformed stochastic CARD equations (2) and (3) and identifying each component with a picture. Free response functions are given

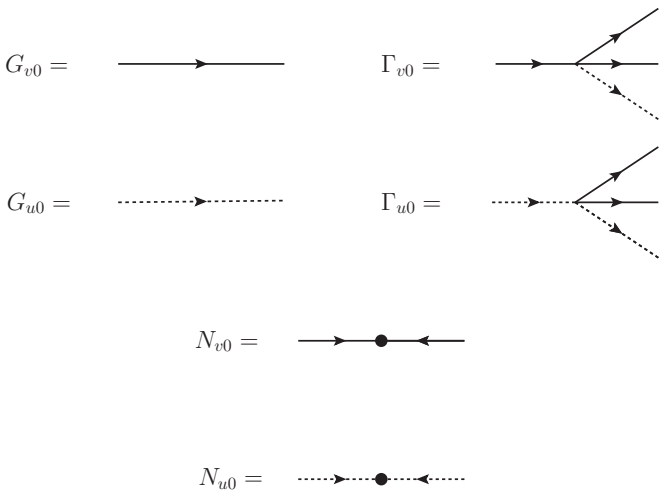

FIG. 5. Feynman rules for the stochastic CARD model corresponding to Eqs. (2) and (3).

by (see Fig. 5):

$$G_{v0}(k) = \frac{1}{D_v|\mathbf{k}|^2 - i\omega + r_v}, \tag{A1}$$

$$G_{u0}(k) = \frac{1}{D_u|\mathbf{k}|^2 - i\omega + r_u}, \tag{A2}$$

with arrows following the sign of the frequency. Tree-level interactions are given by (see Fig. 5):

$$\Gamma_{v0} = -\Gamma_{u0} = \lambda. \tag{A3}$$

The effect of fluctuations is represented by loop diagrams in field theory. Loop diagrams are obtained from noise averaging [cf. Eqs. (5) and (6)]:

$$N_{v0}(k) = 2A_v|\mathbf{k}|^{-y_v}\omega^{-2\theta_v}, \tag{A4}$$

$$N_{u0}(k) = 2A_u|\mathbf{k}|^{-y_u}\omega^{-2\theta_u}. \tag{A5}$$

The components shown in Fig. 5, supplemented with conservation of momentum at each vertex and integration over undetermined momenta, form the basis of perturbation theory. With the appropriate combinatoric factor, they can be used to write down any Feynman diagram for the stochastic CARD model.

APPENDIX B: COMPUTATION OF THE ONE-LOOP CORRECTION TO THE RATE CONSTANT λ

The expression for the one-loop correction to the rate constant is

$$\begin{aligned}\Gamma_\lambda(0) &= -8\lambda^2 A_v \int \frac{d^{d_s}p}{(2\pi)^{d_s}} \int \frac{d\omega}{(2\pi)}\, \omega^{-2\theta_v}|\mathbf{p}|^{-y_v}\left(\frac{1}{D_u|\mathbf{p}|^2 + i\omega + r_u}\right)\left(\frac{1}{D_v|\mathbf{p}|^2 - i\omega + r_v}\right)\left(\frac{1}{D_v|\mathbf{p}|^2 + i\omega + r_v}\right),\\ &= -8\lambda^2 A_v \int \frac{d^{d_s}p}{(2\pi)^{d_s}} \int \frac{d\omega}{(2\pi)}\, |\omega|^{-2\theta_v}|\mathbf{p}|^{-y_v}\left[\frac{1}{|\omega|^2 + (D_v|\mathbf{p}|^2 + r_v)^2}\right]\left[\frac{D_u|\mathbf{p}|^2 + r_u}{|\omega|^2 + (D_u|\mathbf{p}|^2 + r_u)^2}\right].\end{aligned} \tag{B1}$$

Depending on the parameters d_s, y_v, and θ_v, the above one-loop correction may diverge. We regulate the expression by analytically continuing the space dimension to d and the time dimension to z, giving:

$$\Gamma_\lambda(0) = -8\lambda_{(d)}^2 A_v^{(d,z)} \int \frac{d^d p}{(2\pi)^d} \int \frac{d^z\omega}{(2\pi)^z}\, |\omega|^{-2\theta_v}|\mathbf{p}|^{-y_v}\left[\frac{1}{|\omega|^2 + (D_v|\mathbf{p}|^2 + r_v)^2}\right]\left[\frac{D_u|\mathbf{p}|^2 + r_u}{|\omega|^2 + (D_u|\mathbf{p}|^2 + r_u)^2}\right]. \tag{B2}$$

Simple power counting shows that the one-loop correction to the rate constant behaves as

$$\Gamma_\lambda \sim \Lambda^{d-y_v+2z-4\theta_v-6} \sim \Lambda^{2m+2n-4-\epsilon-2\delta}. \tag{B3}$$

From Eq. (B3), we infer that Γ_λ is logarithmically UV divergent for $(m=2,n=0)$ and $(m=1,n=1)$. The first case corresponds to purely spatial noise and is treated in Ref. [24]. The second case is a mixture of spatial and temporal noise. We focus on the latter in the following.

We start by doing the integral over frequency first. Introducing a Feynman parameter in Eq. (B2), we obtain:

$$\Gamma_\lambda(0) = -8\lambda_{(d)}^2 A_v^{(d,z)} \int \frac{d^d p}{(2\pi)^d}\, |\mathbf{p}|^{-y_v}(D_u|\mathbf{p}|^2 + r_u) \int_0^1 dx \int \frac{d^z\omega}{(2\pi)^z} |\omega|^{-2\theta_v} \left[\frac{1}{|\omega|^2 + \Delta(x)}\right]^2, \tag{B4}$$

where

$$\Delta(x) = x(D_v|\mathbf{p}|^2 + r_v)^2 + (1-x)(D_u|\mathbf{p}|^2 + r_u)^2. \tag{B5}$$

Integrating Eq. (B4) using the method of dimensional regularization in the presence of noise [24], we obtain:

$$\Gamma_\lambda(0) = -4\lambda_{(d)}^2 A_v^{(d,z)} K_z \Gamma\left(-\frac{z}{2}+\theta_v+2\right)\Gamma\left(\frac{z}{2}-\theta_v\right) \int \frac{d^d p}{(2\pi)^d} |\mathbf{p}|^{-y_v}(D_u|\mathbf{p}|^2 + r_u) \int_0^1 dx \frac{[\Delta(x)]^{\frac{z}{2}-\theta_v+2}}{2}. \tag{B6}$$

The integral over the Feynman parameter can be done explicitly. The result is

$$\Gamma_\lambda(0) = 4\lambda_{(d)}^2 A_v^{(d,z)} K_z \frac{\pi}{\sin\pi\left(\frac{z}{2}-\theta_v\right)} \int \frac{d^d p}{(2\pi)^d}\, |\mathbf{p}|^{-y_v} \frac{(D_u|\mathbf{p}|^2 + r_u)[(D_v|\mathbf{p}|^2 + r_v)^{z-2\theta_v-2} - (D_u|\mathbf{p}|^2 + r_u)^{z-2\theta_v-2}]}{[(D_v|\mathbf{p}|^2 + r_v)^2 - (D_u|\mathbf{p}|^2 + r_u)^2]}. \tag{B7}$$

To do the integration over momentum, another Feynman parameter must be introduced. Before proceeding, we point out an important subtlety not present in usual quantum field theory computations. The temporal noise correlation exponent θ_v is a parameter and is not specified in Eq. (B7). This implies that the number of factors in the denominator in the integrand and their power depend on θ_v. In practice, the Feynman trick is used to regroup factors in the denominator only. Since θ_v is left unspecified, the number of Feynman parameters needed to regroup the factors in the denominator is ambiguous. This problem is not present in usual quantum field theory computation, since the number of factors is fixed.

To make progress, it is necessary to specify θ_v. As explained in Sec. III A, the first nontrivial case of spatial and temporal noise mixing is $(m=1,n=1)$, implying $z-2\theta_v = 2-\delta$. Plugging this into Eq. (B7) and expanding for small δ, we obtain:

$$\Gamma_\lambda(0) = -8\lambda_{(d)}^2 A_v^{(d,z)} \frac{D_u}{D_v^2 - D_u^2} K_z K_d \int_0^\infty d|\mathbf{p}|\, |\mathbf{p}|^{d-y_v-1} \frac{\left(|\mathbf{p}|^2 + \frac{r_u}{D_u}\right)\left\{\ln\left[\frac{D_v}{D_u}\right] + \ln\left[\frac{(|\mathbf{p}|^2+d_1)}{(|\mathbf{p}|^2+d_2)}\right]\right\}}{(|\mathbf{p}|^2+d_3)(|\mathbf{p}|^2+d_4)}, \tag{B8}$$

where $d_1 = \frac{r_v}{D_v}$, $d_2 = \frac{r_u}{D_u}$, $d_3 = \frac{r_v+r_u}{D_v+D_u}$, and $d_4 = \frac{r_v-r_u}{D_v-D_u}$. There are four contributions to the integrand. Using a cutoff, a tedious calculation shows that only the contribution proportional to $|\mathbf{p}|^2 \ln[\frac{D_v}{D_u}]$ leads to a logarithmic divergence, with all the other terms finite in the UV. Discarding the finite terms, we introduce a Feynman parameter in the remaining term:

$$\Gamma_\lambda(0) = -8\lambda_{(d)}^2 A_v^{(d,z)} \frac{D_u}{D_v^2 - D_u^2} \ln\left(\frac{D_v}{D_u}\right) K_z K_d \int_0^1 dx \int_0^\infty d|\mathbf{p}|\, |\mathbf{p}|^{d-y_v+1} \left[\frac{1}{|\mathbf{p}|^2 + \zeta(x)}\right]^2, \tag{B9}$$

where

$$\zeta(x) = x d_3 + (1-x) d_4. \tag{B10}$$

Integrating Eq. (B9) using the method of dimensional regularization in the presence of noise [24] and expanding around the critical dimension $d_c^\lambda = y_v + 2$, we finally obtain the one-loop correction to the rate constant λ shown in Eq. (17).

[1] L. S. Tsimring, Rep. Prog. Phys. **77**, 026601 (2014).
[2] D. C. Krakauer and A. Sasaki, Proc. R. Soc. Lond. B **269**, 2423 (2002).
[3] J. M. A. Carnall, C. A. Waudby, A. M. Belenguer, M. C. A. Stuart, J. J. P. Peyralans, and S. Otto, Science **327**, 1502 (2010).
[4] J. Ross, Annu. Rev. Biochem **77**, 479 (2008).
[5] W. Horsthemke and R. Lefever, *Noise-Induced Transitions* (Springer, Berlin, 2006).
[6] J. Garcia-Ojalvo and J. M. Sancho, *Noise in Spatially Extended Systems* (Springer, Berlin, 1999).
[7] F. Lesmes, D. Hochberg, F. Morán, and J. Pérez-Mercader, Phys. Rev. Lett. **91**, 238301 (2003).
[8] D. Simakov and J. Pérez-Mercader, J. Phys. Chem. A **117**, 13999 (2013).
[9] H. Sugiura, M. Ito, T. Okuaki, Y. Mori, H. Kitahata, and M. Takinoue, Nat. Commun. **7**, 10212 (2016).
[10] A. M. Turing, Phil. Trans. Roy. Soc. **237**, 37 (1952).
[11] H. Meinhardt, *Models of Biological Pattern Formation* (Academic Press, New York, 1982).
[12] M. C. Cross and P. C. Hohenberg, Rev. Mod. Phys. **65**, 851 (1993).
[13] N. Tompkins, N. Li, C. Girabawe, M. Heymann, G. B. Ermentrout, I. R. Epstein, and S. Fraden, Proc. Natl. Acad. Sci. USA **111**, 4397 (2014).

[14] E. E. Holmes, M. A. Lewis, J. E. Banks, and R. Veit, Ecology **75**, 17 (1994).
[15] J. S. Lowengrub, H. B. Frieboes, F. Jin, Y.-L. Chuang, X. Li, P. Macklin, S. M. Wise, and V. Cristini, Nonlinearity **23**, R1 (2010).
[16] I. R. Epstein and J. A. Pojman, *An Introduction to Nonlinear Chemical Dynamics* (Oxford University Press, Oxford, 1998).
[17] J. E. Pearson, Science **261**, 189 (1993).
[18] J. Higgins, Proc. Natl. Acad. Sci. USA **51**, 989 (1964).
[19] E. E. Sel'kov, Eur. J. Biochem. **4**, 79 (1968).
[20] P. Gray and S. K. Scott, Chem. Eng. Sci. **38**, 29 (1983).
[21] P. Gray and S. K. Scott, Chem. Eng. Sci. **39**, 1087 (1984).
[22] P. Gray and S. K. Scott, J. Phys. Chem. **89**, 22 (1985).
[23] G. Nicolis and I. Prigogine, *Self-Organization in Non-Equilibrium Systems* (Wiley, New York, 1977).
[24] J.-S. Gagnon, D. Hochberg, and J. Pérez-Mercader, Phys. Rev. E **92**, 042114 (2015).
[25] J. S. Gagnon and J. Pérez-Mercader, arXiv:1509.09307.
[26] I. Golding and E. C. Cox, Phys. Rev. Lett. **96**, 098102 (2006).
[27] I. M. Tolic-Norrelykke, E.-L. Munteanu, G. Thon, L. Oddershede, and K. Berg-Sorensen, Phys. Rev. Lett. **93**, 078102 (2004).
[28] B. Hoop and C.-K. Peng, J. Membr. Biol. **177**, 177 (2000).
[29] D. Hochberg, F. Lesmes, F. Morán, and J. Pérez-Mercader, Phys. Rev. E **68**, 066114 (2003).
[30] N. G. van Kampen, *Stochastic Processes in Physics and Chemistry* (North-Holland, Amsterdam, 2007).
[31] U. C. Taüber, M. Howard, and B. P. Vollmayr-Lee, J. Phys. A: Math. Gen. **38**, R79 (2005).
[32] F. Cooper, G. Ghoshal, and J. Pérez-Mercader, Phys. Rev. E **88**, 042926 (2013).
[33] Critical dimensions in the present context are defined as the dimension above which a specific parameter (e.g., r_u, λ) requires renormalization. For example, corrections to r_u are divergent when $d_s \geqslant d_c^{r_u} = y_v + 4\theta_v + 2$ and corrections to λ are divergent when $d_s \geqslant d_c^{\lambda} = y_v + 4\theta_v + 4$ in the CARD model.
[34] M. Egbert and J. Pérez-Mercader, in *Proceedings of the Artificial Life Conference*, edited by C. Gershenson, T. Froese, J. M. Siqueiros, W. Aguilar, E. J. Izquierdo, and H. Sayama (Creative Commons Attribution-NonCommercial-NoDerivatives 4.0 International Public License, 2016), p. 720.
[35] E. Medina, T. Hwa, M. Kardar, and Y. C. Zhang, Phys. Rev. A **39**, 3053 (1989).
[36] A. L. Barabási and H. E. Stanley, *Fractal Concepts in Surface Growth* (Cambridge University Press, Cambridge, 1995).